

ORIGINAL ARTICLE

Open Access

# Characterization of sample preparation methods of NIH/3T3 fibroblasts for ToF-SIMS analysis

Michael A Robinson<sup>1,2</sup> and David G Castner<sup>1,2,3\*</sup>

## Abstract

The information that is obtained from single cells during time-of-flight secondary ion mass spectrometry (ToF-SIMS) analysis is influenced by the method that was used to prepare the cells. The removal of extracellular media before analysis is necessary, but the rinsing technique should not damage the plasma membrane of the cell. The presence of intracellular salts reduced the secondary ion yield an average of 2.6-fold during  $\text{Bi}_3^+/C_{60}^{++}$  depth profiles. Chemical fixation followed by rinsing removed a majority of the intracellular salts, “recovering” the positive secondary ion yields. The formaldehyde-fixation process removed a majority of the intracellular  $\text{Cl}^-$ , but other key anions were not removed in significant amounts. The data presented here is consistent the anion neutralization mechanism largely responsible for the lower ion yields. All of the organic secondary ions that were detected in the freeze-dried cells were also detected in the formaldehyde-fixed cells, suggesting that the fixation process did not remove any molecular species to an extent that is detectable by ToF-SIMS. Compared to freeze dried cells, well preserved, frozen-hydrated cells showed little increase, or a decreased yield, for most low mass ions, but an increased yield for larger mass fragments. This is consistent with a reduced damage cross section at cryogenic analysis temperatures, although proton donation from water and reduction the salt effects in the presence of water likely also play roles. Numerous ions detected from the frozen-hydrated cells were not detected from the freeze dried cells, however many of these ions were attributed to chemical combinations of water, salts and the ammonium acetate rinsing solution.

**Keywords:** ToF-SIMS; Cells; Depth profile; Sample preparation

## Background

Time-of-flight secondary ion mass spectrometry (ToF-SIMS) is a powerful tool that has been used to explore a wide range of biologically relevant samples including: cells and tissues [1-4], lipids [5], proteins on surfaces [6,7], DNA [8,9], drug eluting stents [10,11], explanted biomaterials [12] and decellularized matrix [13]. The unique abilities of ToF-SIMS to acquire a mass spectrum with high mass resolution, as well as produce chemical maps with submicron spatial resolution [14] provides an effective method to probe biological cells and tissues. These strengths, along with the capacity to sputter etch organic material [15,16], may enable the 3D visualization of sub-cellular features including drug, metabolite or

nanoparticle behavior within single cells. There is a continuing need to characterize how diverse sample preparation methods influence the information that is acquired from biological cells [17].

The methods to prepare cells for SIMS analysis can be organized in several ways. A schematic that outlines the most common techniques is shown in Figure 1. They can be separated into one of two fundamental categories: either the cells are dehydrated prior to analysis, or the intracellular water is conserved and the cells are analyzed frozen-hydrated. The methods may also be organized by the mechanism that removes the culture media from a cells' surface before analysis. Either the media is removed with an isotonic rinsing solution, or the cells are freeze-fractured, removing a portion of the cell and all of the media above it, creating a pristine surface for analysis [18,19].

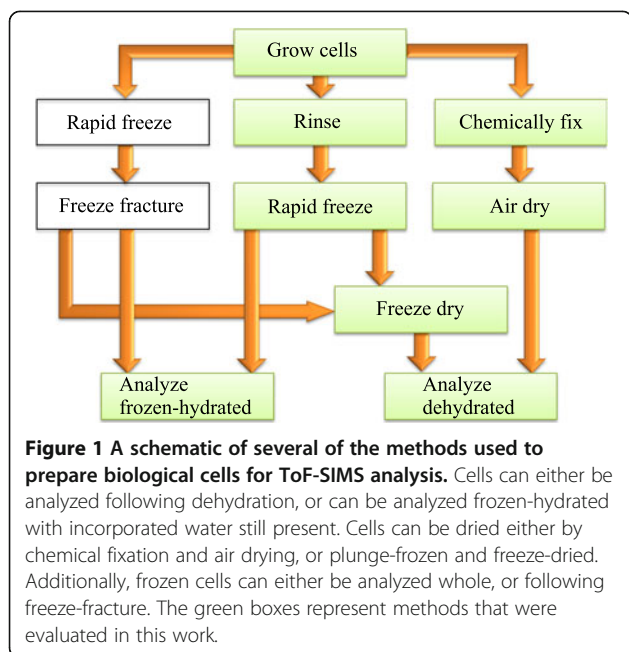
One of the most common constituents in biological specimens are salts, particularly  $\text{Na}^+$ ,  $\text{K}^+$  and  $\text{Cl}^-$ , which

\* Correspondence: castner@uw.edu

<sup>1</sup>National ESCA and Surface Analysis Center for Biomedical Problems, University of Washington, 98195 Seattle, WAUSA

<sup>2</sup>Department of Chemical Engineering, University of Washington, 98195 Seattle, WA, USA

Full list of author information is available at the end of the article



greatly lowered the organic SI yields in rat brain tissue and DPPC films [20], as well as bovine serum albumin and polypeptide films [21]. SI yields were “recovered” by rinsing these samples, which removed most of the salts. On single cells, several rinsing solutions were compared, and it was determined that an isotonic solution (150 mM) of ammonium acetate (AA) best removed extracellular growth medium salts and best preserved cell morphology [22]. Ammonium formate (AF) has worked similarly on cells [23] and tissues [21,24,25]. Interference reflection microscopy determined the volume change of cells immersed in an AF rinsing solution. At 1 minute of immersion time there was a roughly 1.4× volume increase and at 16 minutes the cells had experienced a 2× volume increase. The swelling amount was not sufficient to rupture the plasma membrane and many cells were viable after a 16 minute immersion [24].

Breitenstein *et al.* used glutaraldehyde-fixation to image single NRK cells in 3D and argued the merits of chemical fixation as a method to prepare cells for ToF-SIMS analysis [26,27]. The key conclusions included glutaraldehyde-fixation did not cause significant shrinkage of the cell, that cellular compartments remained intact following fixation, and that the distribution of most molecular chemical components (proteins, DNA, lipids) was conserved.

The effects of cryofixation and freeze-drying, as well as various chemical fixations on the morphology and SI yields from the plasma membrane of human fibroblasts were compared by Malm *et al.* [24]. While the cells’ extracellular fine structure was better preserved using

chemical fixation, the native intracellular  $K^+/Na^+$  ratio was not maintained. The permeability of the plasma membrane to mobile ions was also utilized in early ion microprobe experiments which tested practical ion yields [28]. Intracellular  $K^+/Na^+$  ratios have been used as one indicator to determine the quality of cell preservation. Popularized in the SIMS community by Chandra *et al.*, this ratio has been used to identify healthy cells from damaged ones [18,29,30], where a healthy cell has a high  $K^+/Na^+$  ratio. Membrane damage, caused by either the freezing or drying processes resulted in increased permeability to diffusible ions and the loss of this natural gradient. Many of these issues were discussed by Clerc *et al.* with an emphasis on mapping intracellular drugs and nuclear medicine compounds [31]. A major assertion was that cryofixation methodologies are required when examining highly mobile ions and chemical fixation should only be employed when studying molecules fixed to cell structures.

The investigation of frozen-hydrated (FH) cells with ToF-SIMS may be beneficial for several reasons. First, it allows a cell to be studied in its most native state. Rapid freezing provides a “snapshot” of the cell at a given instant, arresting all biological activity on a millisecond time scale [32]. Dehydration may cause cells to shrink or crack, may redistribute membrane lipids and/or cause plasma membranes to rupture [22,24,33]. However shrinking was not reported [26] and membrane lipid distributions were preserved using glutaraldehyde-fixation [34]. At cryogenic temperatures, depth resolution and SI yield were improved in depth profiling polymers, partly by reducing sputter-induced topography. [35,36]. Several studies have reported increased SI yields in FH analyses, and suggested that the increased yield resulted from proton donation from incorporated water molecules to neutral species [37,38]. Incorporated water during FH analysis has also alleviated the reduction of SI yields caused by KCl-doped arginine films, restoring yields to those that were acquired on undoped films [20]. Cryogenic analysis reduced the damage cross section of primary ions, which improved the SI yields of larger molecular weight ions in polypeptide films [37].

When cells are analyzed FH with ToF-SIMS, a majority of surface water must be removed due to the 1–2 nm surface sensitivity it provides. A practical method to remove this surface water is *in situ* sublimation [38–40]. This is generally achieved by slowly warming the sample stage from cryogenic temperature to  $-80^{\circ}C$ , effectively freeze-drying the sample for a short period of time. With FH cell analysis, sublimation is often a necessary step to remove any rinsing solution left over from the removal of the culture media.

Instrumentation developments that specifically addressed improving FH SIMS experiments include Ionoptika’s J105,

which allows for the *in-situ* freeze fracturing of a frozen cells under vacuum [41]. A cryomicrotome was attached to a ToF-SIMS instrument to serial section frozen tissue *in situ* and analyze the fresh face of sequential tissue slices [42]. Also, recently an *in-situ* freeze fracture device was adapted from the J105 freeze fracture system to work on an ION-TOF IV cold stage [43].

As summarized above, there is significant interest and challenges in using different sample preparation procedures for ToF-SIMS imaging of biological cells. The current study provides a comprehensive comparison of the mass spectral information that was obtained from formaldehyde-fixed cells, cryofixed and dehydrated cells, and frozen-hydrated cells. The surface spectra were obtained from cells that were prepared using each preparation method and examined. The secondary ion yields from depth profiles of the chemically fixed cells were compared to freeze-dried cells. A second SI yield comparison was made between freeze-dried cells and frozen-hydrated cells. All organic ions in all depth profiles were investigated. While there have been studies in the past that have examined SI yields as a function of cell preparation method [24,33], this is the most complete analysis to date. Additionally, several peaks from the frozen-hydrated analyses were identified that were not detected from the dried cells. This work offers additional insight into which are the primary mechanisms of SI yield enhancement and degradation during ToF-SIMS depth profiling of biological cells.

## Methods

### Cell seeding

NIH/3T3 fibroblasts were seeded onto 1 cm × 1 cm silicon chips [44] at densities between 40,000-100,000 cells and grown for 24–48 hours in Eagle's Dubelco's Modified Essential Medium (Invitrogen, San Diego, CA) supplemented with 10% fetal bovine serum (Thermo Scientific, Erie, PA) and 1% antibiotic/antimycotic (Invitrogen, San Diego, CA). Prior to cell seeding the silicon chips were cleaned with 2x sequential five-minute sonications in dichloromethane, acetone and methanol and stored in a laminar hood until cell seeding.

### Ammonium acetate rinsing solution

Ammonium acetate (AA) (Sigma, St. Louis, MO) was dissolved in 18 MΩ water to form a 150 mM solution, and was brought to pH 7.4 with 1 M ammonium hydroxide [22].

### Rinsing, plunge freezing and freeze-drying of cells

Cells on silicon chips were gently rinsed in 150 mM AA for 30 seconds by slowly dipping the silicon chip in the solution followed by minimal movement of the sample in the rinsing solution. Excess liquid was removed by

touching the edges of the chip with a Kimwipe. The sample was then rapidly submerged in liquid ethane (produced by leaking ethane gas into a liquid nitrogen cooled plastic beaker) and quickly transferred to liquid nitrogen (LN<sub>2</sub>). While under LN<sub>2</sub>, the chips were placed into small glass test tubes, and the tops were covered with aluminum foil with a small hole. These test tubes were placed into a pre-cooled freeze-dry flask (−80°C freezer overnight), while the chips were still submerged in LN<sub>2</sub>. The flask was attached to a manifold freeze drier (SP Scientific, Warminster, PA) and a vacuum was established. The samples dried overnight, and then were immediately placed into the ToF-SIMS instrument for analysis.

### Chemical fixation

Cells on silicon chips were rinsed briefly in the AA solution and placed into a 4% formaldehyde (Thermo Scientific, Erie, PA) in PBS buffer (EDS Chemicals) solution at room temperature for 30 minutes. The samples were removed and rinsed for 60 seconds in water. Excess liquid was removed from the samples by touching the edges with a Kimwipe, and then they were air dried overnight in a laminar flow hood. The samples were analyzed the following morning.

### Frozen-hydrated: preparation of cells and analysis

Samples were prepared in a manner similar to that described in Piwowar *et al.* [45]. Cells on silicon chips were rinsed and plunge frozen as described above. Prior to freezing, it is important to reduce the thickness of the liquid layer to a minimum in order to ensure the best freezing results. After cryofixation in liquid ethane, the samples were transferred to LN<sub>2</sub> until placement onto the ToF-SIMS cold stage. The cold stage was pre-cooled to −160°C at 10<sup>−7</sup> mbar in the loading chamber, then vented to atmosphere to allow for the placement of the sample. The sample was rapidly transferred from under liquid nitrogen onto the cold stage, where it was held onto the stage by a clip. The cold finger was immediately brought into contact with the cold stage and the loading chamber was immediately pumped down to 5×10<sup>−7</sup> mbar. The maximum temperature of the cold stage was −85°C during the entire process, as measured by a thermocouple mounted to the surface of the stage. After the loading chamber was evacuated the sample stage was cooled to −130°C before warming at a rate of 5°C/min to −80°C [38]. The stage was held at −80°C for 30 minutes to sublimate the excess water from the surface of the cells. After the sublimation, the stage was cooled to −160°C and transferred into the analysis chamber. All analyses were performed with the stage temperature at −130°C. Cells maintained a high K<sup>+</sup>/Na<sup>+</sup> ratio, as shown in Additional file 1: Figure S1.

### ToF-SIMS

Positive and negative secondary ion spectra were collected with an ION-TOF TOF SIMS 5–100 instrument (ION-TOF, Münster, Germany), using a pulsed 25 keV  $\text{Bi}_3^+$  primary ion beam. Samples were sputtered using a 20 keV  $\text{C}_{60}^{++}$  beam. The Bi and  $\text{C}_{60}$  beams were oriented  $45^\circ$  to the surface normal. Depth profiles were acquired using the high mass resolution mode ( $m/\Delta m = 7000$  at  $m/z$  27) in the interlaced mode (one analysis scan per sputter cycle) with a  $\text{Bi}_3^+$  current of 0.15 pA and an analysis area of  $500 \times 500 \mu\text{m}^2$ . The  $\text{C}_{60}^{++}$  current was kept between 0.3–0.35 nA and a sputter area of  $700 \times 700 \mu\text{m}^2$  was used for all depth profiles. All depth profiles were acquired for 1000 seconds, one shot/pixel and contained  $128 \times 128$  pixels. Positive ion spectra were mass calibrated using the  $\text{CH}_3^+$ ,  $\text{C}_2\text{H}_3^+$ ,  $\text{C}_3\text{H}_5^+$ ,  $\text{C}_3\text{H}_3\text{O}^+$ , and  $\text{C}_7\text{H}_7^+$  peaks. Negative ion spectra were mass calibrated using the  $\text{CH}^-$ ,  $\text{OH}^-$ ,  $\text{PO}_2^-$ , and  $\text{PO}_3^-$  peaks. Secondary ions were collected over a range of 0–860  $m/z$ . Low energy electrons were flooded onto the sample to compensate for charge buildup on the surface. Some data was collected in the .RAW format using the IONTOF Version 4 software and subsequently converted into the .itm raw data format (IONTOF Surface Lab 6). All data was analyzed using the IONTOF Surface Lab 6 software.

Regions of interest (ROI's) for the cells were chosen in all analyses by thresholding the “totalcounts” image. The signal from the cells was significantly higher than from the substrate. Regions were chosen so that a minimum of substrate would be analyzed during the depth profiles. The SI intensities from the depth profiles were normalized by the primary ion dose to allow direct comparison. Peak lists were created by overlaying representative spectra from each of the preparation methods and using manual peak selection. Known substrate, salt and salt adduct peaks were excluded from the peak lists.

### Results and discussion

The purpose of these experiments was to examine how various methods of sample preparation affected the chemical information obtained from single cells, with an emphasis on SI yields from depth profiles. This work compares cells that were prepared by formaldehyde-fixation (FF), plunge freezing and freeze-drying (FD), and plunge freezing with frozen-hydrated analysis (FH). This is important for 3D ToF-SIMS imaging, where SI intensities of organic species often quickly decrease due to sputtering induced damage [46].

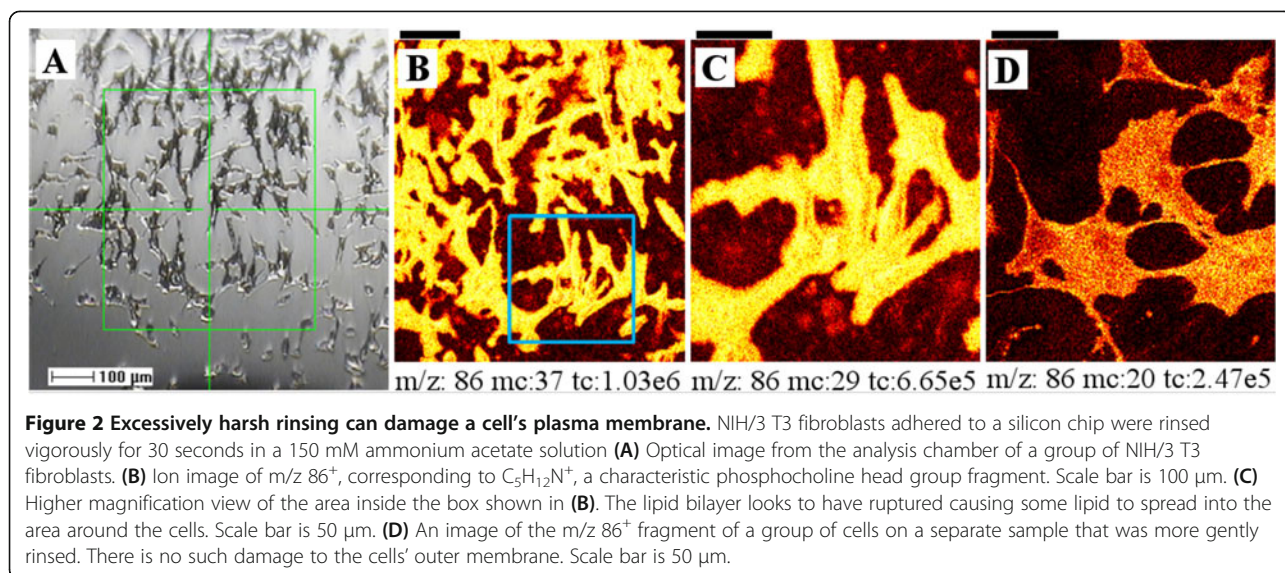
#### Proper rinsing of cells

The removal of excess media from the surface of cells prior to analysis is an important step in the preparation protocol for ToF-SIMS analysis [22,24]. An improper

rinsing technique can stress the plasma membrane such that it is damaged, as depicted in Figure 2. In an effort to completely remove extracellular media salts from the surface of the cells prior to cryofixation, the sample was immersed in a rapidly stirred AA solution. The cells were submerged for 30 seconds, plunge frozen and freeze dried. An optical image from the analytical chamber of the ToF-SIMS instrument is shown in Figure 2A, where a group of fibroblasts is displayed. A high spatial resolution image of the characteristic phosphocholine (PC) head group fragment at  $m/z$  86 ( $\text{C}_5\text{H}_{12}\text{N}^+$ ) is shown in 2B, and 2C is a zoomed-in area of a subset of cells from 2B (blue square). Comparing the lipid distribution from 2C to the optical image from 2A, the plasma membranes appear “smeared”. Shear stress on the membrane from the rapidly moving fluid may have caused this disruption. In Figure 2D a cluster of cells from a separate sample are shown that were gently dipped into a stagnant rinsing solution for 30 seconds and then plunge frozen and freeze dried. No smearing of the cell membrane is visible and sufficient salts have been removed to acquire a meaningful spectrum. Thus, to rinse cells without causing plasma membrane smearing, samples should be gently dipped into a rinsing solution for 30–60 seconds. Vigorous stirring should be avoided.

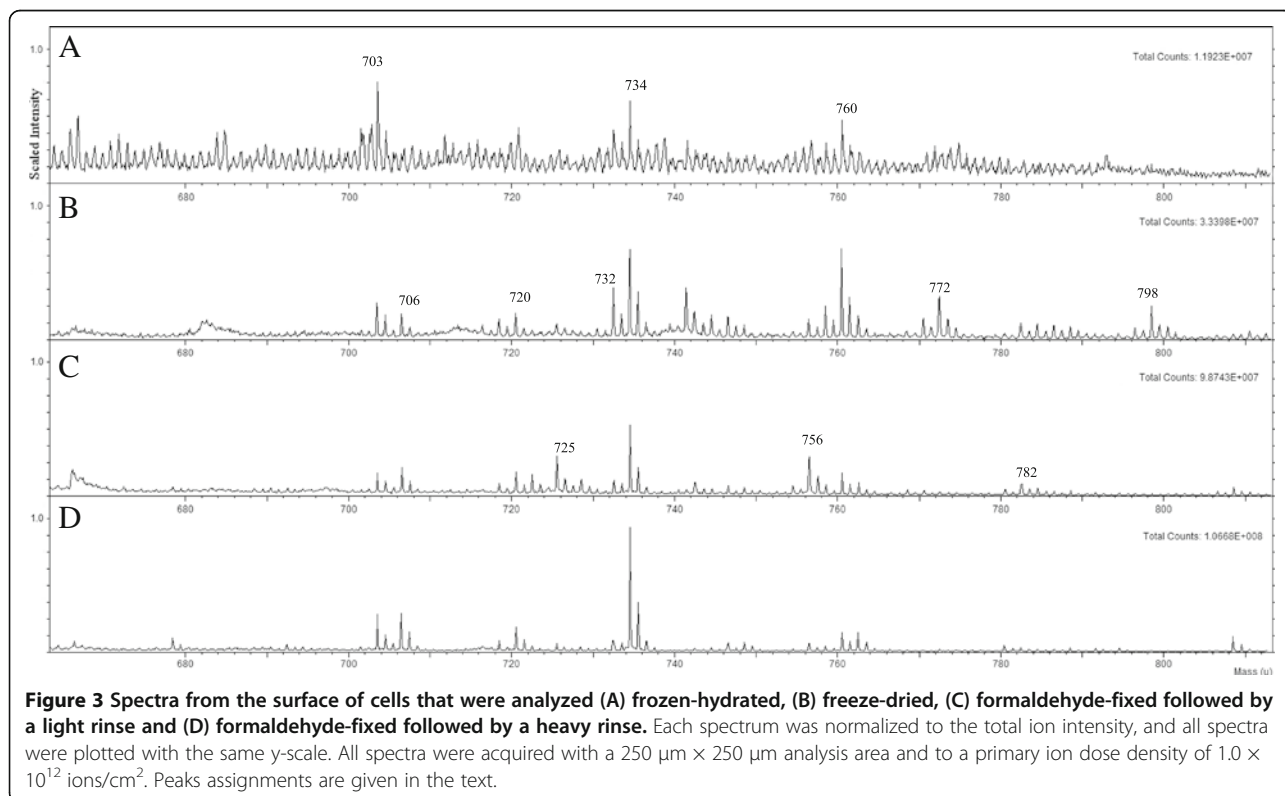
#### Spectra from cell surfaces

Figure 3 shows the positive SI spectra between  $m/z$  660–810, collected from the surface of NIH/3T3 fibroblasts that were analyzed after the following preparation methods: A) FH, B) FD, C) FF with a light rinse after fixation and D) FF with a heavy rinse after fixation. Each spectrum was normalized to the total counts detected and plotted on the same y-scale. The ions at  $m/z$  703, 732, 734 and 760 were detected in the spectra from cells using each of the preparation methods. These ions were identified as sphingomyelin SM(34:1) [47], glycerophosphocholine PC(32:1), PC(32:0) [48], and PC(34:1) [49]. The peak at  $m/z$  762.2 was identified as PC(34:0). An unidentified peak at  $m/z$  720.5 was present in each of the spectra. An unidentified peak at  $m/z$  706.5 was present in all but the FH spectrum. The  $\text{K}^+$  adducts of SM(34:1), PC(32:1), PC(32:0) and PC(34:1) were detected at  $m/z$  741, 770, 772 and 798, whereas the  $\text{Na}^+$  adducts of these lipids were detected at  $m/z$  725, 754, 756 and 782, respectively [25]. The  $\text{K}^+$  adducts were not detected in high levels in either of the FF samples, consistent with previous experiments that showed a majority of  $\text{K}^+$  was removed during the fixation process [24]. The FF sample that was not rinsed well after fixation had the highest intensity of  $\text{Na}^+$  adduct ions, as expected since  $\text{Na}^+$  is a major component of the PBS fixation buffer.



The FH and FD spectra were more similar to one another than to the FF spectra, however all four spectra contained the same major peaks. The largest differences between the spectra from the FD (3B) and FF (3D) cells were the lowered intensity of PC(34:1) and PC(32:1), and the increased intensity of PC(32:0) in the FF spectrum. This is consistent with previous results where the normalized intensity of PC(34:1) was lower in glutaraldehyde-fixed cells compared to

cryofixed and FD cells [24]. The SM(34:1) ion had a comparable intensity to the PC(32:0) and PC(34:1) peaks in the FH spectrum, whereas in all three spectra of dried cells the SM(34:1) intensity was lower than the PC peaks. These differences in the spectra may have been caused by the increased disorganization of the plasma membrane as the cells shifted from fully hydrated (most native), to freeze dried, to formaldehyde-fixed (least native).



The spectrum from the FH cells was similar to that of the FD cells likely because the FH cells were subjected to a  $-80^{\circ}\text{C}$  environment for a short time to sublime excess surface water. Although a thin layer of water was redeposited onto the surface after this sublimation period (Additional file 2: Figure S2 C), this would likely not reverse any re-organization of the membrane caused by the initial freeze-drying, although it likely would increase ion yields. An ideal preparation to study the plasma membrane would stop the sublimation process with a 1 nm water layer on the sample surface [50]. Perhaps an easier method, although one that was not explored in this work, would be to stop the sublimation with a surface water layer between 10 – 100 nm, and then use cluster sputter etching ( $\text{C}_{60}$  or large argon clusters) to remove the remaining water to reach the plasma membrane. The sublimation step is not necessary for freeze-fracture experiments on single cells because a pristine intracellular surface is produced by the fracture process [18,51]. Due to the difficulty of producing a uniform, thin ice layer, freeze-fracturing may be a better choice for the FH analysis of cells' plasma membranes.

Chemical fixation has caused the plasma membrane to become disorganized in some instances, but not in others. Recent work that imaged the sphingomyelin domains in NIH/3T3 cells used glutaraldehyde-fixation and observed that the plasma membrane was not disorganized [34]. A glutaraldehyde-fixed hTERT-BJ1 fibroblast cell did not show signs of membrane rupture in the  $m/z$  184<sup>+</sup> signal [24]. Cells that were fixed with formalin and freeze dried [33], as well as NIH/3T3 fibroblasts fixed with formaldehyde [52] did show evidence of plasma membrane rupture. Glutaraldehyde can cross-link the free amine group in phosphoserine and phosphoethanolamine, prominent components of the inner leaflet of the plasma membrane, while formaldehyde cannot. This may be the explanation for the disorganized plasma membranes seen when formaldehyde was used as the fixating agent.

#### Comparing the depth profiles of FD and FF cells

One of the most exciting prospects of biological sample analysis with ToF-SIMS is depth profiling and the accurate 3D reconstruction of mass-spectral data sets [33,52]. Low ion yields are the largest hurdle to overcome when acquiring 3D images [53], as there often isn't enough signal intensity for most organic ions of interest to produce a meaningful reconstruction. Salts played a significant role in the suppression of SI yields obtained from depth profiles of rat brain tissue [21] and polypeptide films [20]. To test the extent to which positive SI intensities could be "recovered" by the removal of a majority of intracellular salts ( $\text{Na}^+$ ,  $\text{K}^+$ , and  $\text{Cl}^-$ ), NIH/3T3 fibroblasts were prepared using two methods and depth

profiles were acquired. In the first method, cells were plunge-frozen in liquid ethane and freeze dried, which preserved the native intracellular gradients of mobile species. In the second method, cells were fixed with formaldehyde, rinsed to remove buffer salts, and air dried. Chemical fixation will disrupt the native concentration gradients of mobile ions [24,31], and as such, with heavy rinsing, can be used as a sample preparation method that produces single cells with minimal intracellular salts.

The possibility that intracellular molecules were removed during FF process was examined. The membrane is permeabilized to small molecules during the fixation procedure. Therefore, it is possible some of the intracellular molecules could pass through the permeabilized membrane and be removed during the rinsing step. However, all of the positive ions detected from the FD cells were also detected in the FF cells. Thus, for the instrument parameters and the preparation methodologies used in this study, no removal of intracellular organic ions was detected.

311 common ions were present in the spectra obtained from the two preparation methods. The fold difference in the average, normalized intensity (FF/FD) for each ion is shown in Figure 4. The horizontal red line at 1 indicates the same normalized intensity was collected for a given ion from both preparation methods. The normalized intensities of the selected SIs were higher from the depth profiles of FF cells compared to the FD cells. Of the 311 peaks, 14.6% of the ions had an increase in intensity of less than 2 $\times$ , 56.3% increased between 2 $\times$  and 3 $\times$ , and 29.1% increased greater than 3 $\times$  compared to the FD cells. For the entire peak set, the FF cells had an average increased intensity of 2.6 fold compared to the FD cells. The numerical values of the fold differences of all 311 SIs are shown in Additional file 3: Table S1. Two-tail student's *t*-tests assuming unequal variance were conducted to determine if the intensity differences were statistically significant. The results are shown in Additional file 3: Table S1. Using a *p*-value threshold of 0.05, 309 of the 311 ions had statistically significant intensity differences. The two ions that did not exhibit a significant intensity difference were  $\text{C}_4\text{H}_{12}\text{N}^+$  and  $\text{C}_5\text{H}_{14}\text{NO}^+$  at  $m/z$  74.10<sup>+</sup> and 104.11<sup>+</sup>.

The intensities of the characteristic PC fragments at  $m/z$  58<sup>+</sup>, 86<sup>+</sup>, 104<sup>+</sup>, 125<sup>+</sup>, and 184<sup>+</sup> [54,55] were among the ions with the lowest fold increase. They had fold increases at or below 2.1 (color-coded yellow in Additional file 3: Table S1) compared to the 2.6 fold average increase, and include the ions with the lowest ( $m/z$  104.11<sup>+</sup>) and third lowest increase ( $m/z$  86.06<sup>+</sup>). The intensity of hydrocarbon fragments (color-coded blue) generally increased less than nitrogen- and oxygen-containing fragments. The SIs associated with proteins [56,57], were often nitrogen-

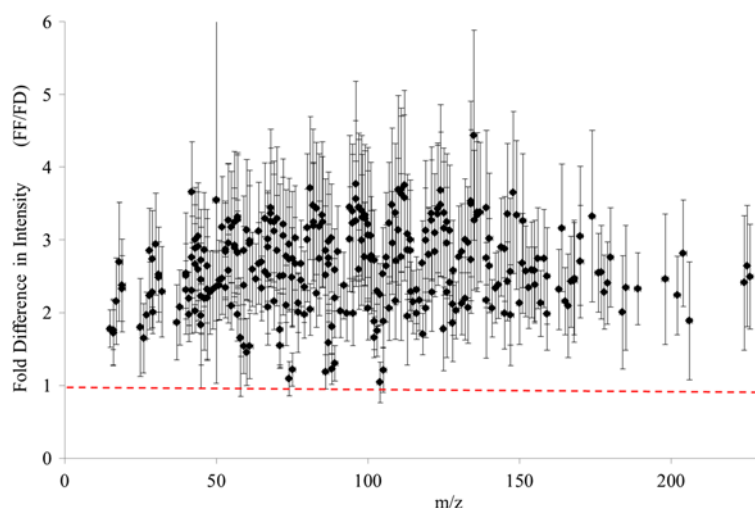


**Figure 4** Depth profiles were acquired from cells that were freeze-dried (FD) and from those that were formaldehyde-fixed (FF). 311 ions were selected that were detected in the spectra of both sample types. The intensity of each ion was summed over the entire depth profile. Intensity values for each ion were averaged and normalized to the total ion dose. For a given ion, the average intensity from the FF cells was divided by the average intensity from the FD cells. The fold difference is plotted on the y-axis as a function of  $m/z$ . The red dotted line signifies a (FF/FD) intensity of 1. Error bars signify one standard deviation. All depth profiles were acquired for 1000 seconds, with a  $500\ \mu\text{m} \times 500\ \mu\text{m}$  analysis area and a  $700\ \mu\text{m} \times 700\ \mu\text{m}$  sputter area. For the FD cells,  $n = 10$ , from four total samples and three separate data acquisition sessions. For the FF cells,  $n = 7$ , from three total samples and three separate data acquisition sessions.

containing (color-coded green) and generally had a larger fold increase than the hydrocarbon and lipid-associated ions. SIs containing oxygen, but not nitrogen (color-coded red) did not display a clear trend, however they also generally had higher fold increase than the lipid and hydrocarbon ions. Despite the nitrogen and/or oxygen content, the fragments originating from PC did not exhibit a large increase. A similar finding was reported when the  $m/z\ 86^+$  SI intensity did not change appreciably in depth profiles of rat brain tissue that had been rinsed versus not rinsed, whereas the  $m/z\ 184$  did have an increased intensity when the tissue was rinsed [21].

It was previously hypothesized that the neutralization of positive SIs by  $\text{Cl}^-$  anions in KCl-doped polypeptide films was the major mechanism of the lowered observed SI yields versus un-doped films [20]. The strongest piece of evidence that supported this mechanism over the others that were proposed was the decreased yield of *all* observed organic ions from the films in the presence of  $\text{Cl}^-$  containing salts. In this work, a similar decrease in all organic SI yields was observed in the FD cells compared to the FF cells. The relative, normalized SI signals from the  $\text{OH}^-$ ,  $\text{CN}^-$ ,  $\text{Cl}^-$ ,  $\text{CNO}^-$ ,  $\text{PO}_2^-$  and  $\text{PO}_3^-$  anions are plotted in Figure 5. These were examined to determine if they could explain the trend observed in Figure 4. The  $\text{Cl}^-$  anion had a statistically significant, higher SI intensity in the FD cells compared to the FF cells. The other five anions except  $\text{Cl}^-$  did not have a statically different SI intensity between the FD and FF cells, although all of the anions except  $\text{PO}_3^-$  had higher mean intensities. This

suggests that the anion neutralization mechanism hypothesized by Piwowar *et al.* is the underlying mechanism that caused the decreased SI intensities acquired from the FD cells, and that the removal of the intracellular  $\text{Cl}^-$  by fixation and rinsing can improve SI yields.

Depth profiles from freeze-dried and formaldehyde fixed cells are shown in Additional file 2: Figure S2 A and B, respectively, depicting the Poisson-corrected intensity of selected secondary ions as a function of  $\text{C}_{60}^{++}$  sputter time. The depth profiles were normalized to the  $\text{Bi}_3^+$  ion dose. The  $\text{NH}_4^+$ ,  $\text{Na}^+$ ,  $\text{K}^+$ ,  $\text{C}_3\text{H}_8\text{N}^+$ ,  $\text{C}_4\text{H}_8\text{N}^+$ ,  $\text{C}_5\text{H}_{12}\text{N}^+$  and  $\text{C}_5\text{H}_{15}\text{PNO}_4^+$  ions are displayed. For the organic molecules, the line shapes from the two depth profiles look qualitatively similar. In both cases, the initial intensities of the organic molecules were the highest, followed by a quick decay with increasing sputter dose. The normalized intensities of the organic molecules are also all higher throughout the depth profile of the formaldehyde-fixed cells, consistent with the data presented in Figure 4.

#### Comparing the depth profiles of FD and FH cells

There was a larger difference between the summed depth profile spectra of the FH cells and the FD cells than between the FF and FD cells. It was more difficult to compare the spectra of the FH cells to the FD cells than the spectra of the FD to the FF. The mass resolution was, generally, worse in the spectra of FH cells than the dried cells, which made the selection of peaks present in both types of spectra difficult. One

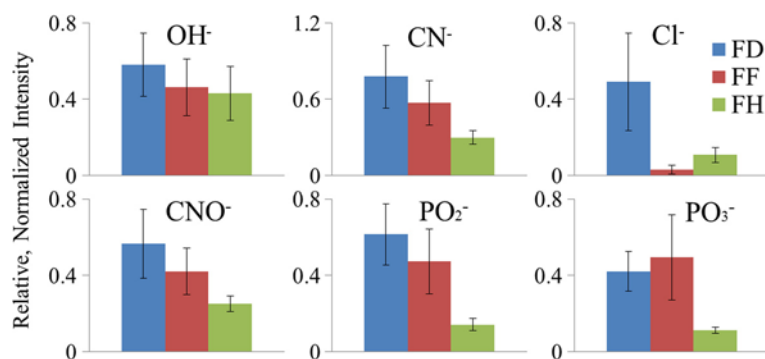


**Figure 5** Depth profiles were acquired from cells that were freeze-dried (FD, blue bars), formaldehyde-fixed (FF, red bars) and frozen-hydrated (FH, green bars). The average, normalized intensity of the OH<sup>-</sup>, CN<sup>-</sup>, Cl<sup>-</sup>, CNO<sup>-</sup>, PO<sub>2</sub><sup>-</sup>, and PO<sub>3</sub><sup>-</sup> ions were summed over the entire depth profile and plotted. Intensity values for each ion were normalized to the total ion dose. Error bars signify one standard deviation. All depth profiles were acquired for 1000 seconds, using a 500 μm × 500 μm analysis area and a 700 μm × 700 μm sputter area. For the FD cells, n = 10, from four total samples and three separate data acquisition sessions. For the FF cells, n = 7, from three total samples and three separate data acquisition sessions. For the FH cells, n = 11, from three total samples and three separate data acquisition sessions.

explanation is that the Bi<sub>3</sub><sup>+</sup> analysis source was optimally tuned in between analyses of the dry samples, whereas the Bi<sub>3</sub><sup>+</sup> source could only be tuned 2–3 hours before the analysis of the FH samples began, and not during the data acquisition. A second possible explanation focuses on the dehydration effect of cells. Full dehydration can collapse cells, reducing the height of dried cells compared to the hydrated form. The mass resolution obtained by the ION-TOF V instrument is sensitive to height variations, and since the hydrated cells were taller than the dried cells (AFM micrographs, data not shown), the mass resolution in the spectra of the FH cells may have been reduced compared to the flatter, dehydrated cells.

There were numerous peaks in the spectra from FH cells that were not detected, or detected in very low amounts, in the spectra of the FD cells. These ions are listed in Additional file 4: Table S2 with possible chemical identifications. No peak assignments indicate that a rational identification was not determined. A majority of these “new” peaks were assigned combinations of water, the ammonium acetate rinsing solution, and intracellular salt ions. In depth profiles of FH samples, water clusters such as H<sub>3</sub>O-H<sub>2</sub>O<sup>+</sup> and H<sub>3</sub>O-(H<sub>2</sub>O)<sub>2</sub><sup>+</sup> at m/z 37 and 55 initially decreased in intensity and then increased with time (data not shown). The initial decrease was attributed to the removal of surface water, which adsorbed after the initial sublimation step. Water clusters with Na<sup>+</sup> and K<sup>+</sup> adducts were also detected, e.g. K-H<sub>2</sub>O<sup>+</sup>. Many of the ions detected in the FH but not FD spectra included NH<sub>3</sub><sup>+</sup> or NH<sub>4</sub><sup>+</sup> in their compositions, which can be attributed at least in part due to the AA rinsing solution. Examples include the ions detected at m/z 52.09<sup>+</sup> and 53.07<sup>+</sup>, which were identified as (NH<sub>3</sub>)<sub>2</sub>-NH<sub>4</sub><sup>+</sup> and (NH<sub>3</sub>)<sub>2</sub>-H<sub>3</sub>O<sup>+</sup>. The intensity of the m/z 53.07<sup>+</sup> fragment

decreased rapidly initially, in a similar fashion to the other water clusters. Since not all of the ions could be identified with reasonable certainty, it is possible that some of them are more biologically relevant than simply being water- or salt-containing.

The fold difference between the normalized intensities of the 137 SIs detected from both the FH and FD samples are shown in Figure 6. The SIs with a higher intensity from the FH cells were plotted in the top half of Figure 6 using a positive fold increase (FH/FD > 1), whereas the SIs with a higher intensity from the FD cells were plotted in the bottom half of Figure 6 using a negative fold increase (FH/FD < -1). The red, dashed lines at 1 and -1 indicate a ratio of 1, and thus no intensity difference. The numerical values of the fold difference of all ions are shown in Additional file 5: Table S3. Two-tail student's *t*-tests were performed assuming unequal variance to determine if the intensity differences were statistically significant. A majority of SIs with m/z < 80 had higher intensities from the FD cells. The low mass SIs that had a statistically significant increased intensity in the FH spectra were CH<sub>3</sub><sup>+</sup>, CH<sub>4</sub>N<sup>+</sup>, CH<sub>3</sub>O<sup>+</sup>, CH<sub>5</sub>N<sup>+</sup>, C<sub>2</sub>H<sub>2</sub>O<sup>+</sup>, CH<sub>4</sub>NO<sup>+</sup>, C<sub>2</sub>H<sub>8</sub>N<sup>+</sup>, C<sub>3</sub>H<sub>7</sub>N<sup>+</sup>, C<sub>3</sub>H<sub>5</sub>O<sup>+</sup>, and possibly C<sub>3</sub>H<sub>3</sub>Na<sup>+</sup>. All of these ions except CH<sub>3</sub><sup>+</sup> possibly contain an NH<sub>4</sub><sup>+</sup>, H<sub>2</sub>O<sup>+</sup> or H<sub>3</sub>O<sup>+</sup> group. An increased SI intensity was obtained for larger masses in FH samples compared to the FD samples. An increase in the FH/FD ratio with increasing mass of the fragment was observed for the PC fragments at m/z 86<sup>+</sup>, 104<sup>+</sup>, 125<sup>+</sup>, 166<sup>+</sup>, 184<sup>+</sup> and 224<sup>+</sup> (labeled with red arrows in Figure 6). The m/z 86 fragment had the lowest fold difference (-1.9) for FD/FH. This value increased for the larger fragments at m/z 104<sup>+</sup> and 125<sup>+</sup>, although the intensities from the FD cells were still higher than from the FH cells. Of the PC-related ions, the m/z 166 fragment had a SI yield higher

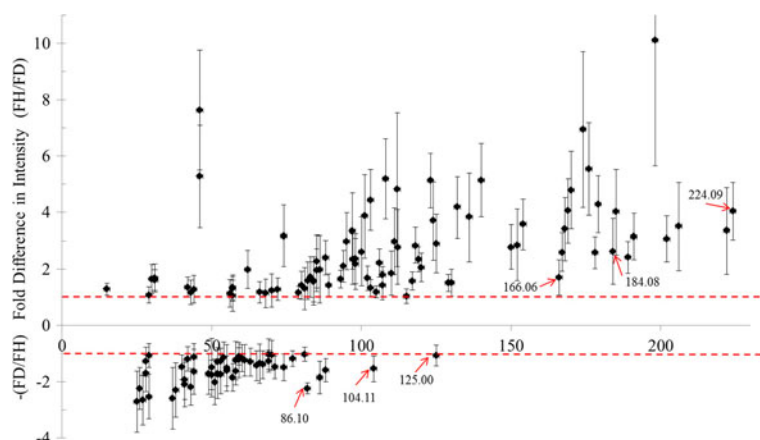


**Figure 6** Depth profiles were acquired from cells that were freeze-dried (FD) and from those that were frozen-hydrated (FH). 137 ions were selected that were detected in the spectra of both sample types. The intensity of each ion was summed over the entire depth profile. Intensity values for each ion were averaged and normalized to the total ion dose. For a given ion, the average intensity from the FD cells was divided by the average intensity from the FH cells. If this ratio was below one, the  $-(FD/FH)$  ratio was used instead. The fold difference is plotted on the y-axis as a function of  $m/z$ . The red dotted lines signify  $(FH/FD)$  and  $(FD/FF)$  intensities of 1. Error bars signify one standard deviation. All depth profiles were acquired for 1000 seconds, with a  $500\ \mu\text{m} \times 500\ \mu\text{m}$  analysis area and a  $700\ \mu\text{m} \times 700\ \mu\text{m}$  sputter area. For the FD cells,  $n = 10$ , from four total samples and three separate data acquisition sessions. For the FH cells,  $n = 11$ , from three total samples and three separate data acquisition sessions.

in the FH cells, and the  $m/z\ 224^+$  had the greatest fold increase. In fact, all selected SIs above  $m/z\ 89^+$  except the  $m/z\ 104^+$  and  $125^+$  (both PC fragments) had an increased intensity from the FH cells compared to the FD cells.

The SI yield results described above are in agreement with previous findings from cryogenic depth profiling experiments of polypeptide films. An increased  $[M + H^+]$  intensity in the peptide films was observed when they were cooled from room to cryogenic temperatures during analysis, although there was little to no increase in lower molecular weight fragments [37]. The increased molecular ion signal was attributed to a decreased damage cross-section, produced by the presence of surface water and cryogenic temperatures. More recent work compared the spectra following  $C_{60}$  sputter etching from within chemically-fixed, freeze-dried HeLa-M cells to FH cells and observed higher yields for the characteristic DNA peaks at  $m/z\ 136^+$ ,  $152^+$ , as well as the PC peak at  $m/z\ 184^+$  [33]. In that study case, lower mass peaks were not investigated. The results presented in Figure 6 from depth profiles of NIH/3T3 fibroblasts support the hypothesis that the primary mechanism of increased molecular SI signals result from a decreased damage cross section produced by cryogenic temperatures. The other mechanisms that have been proposed as a source of increased yields from FH analysis, namely proton donation [58] and amelioration of anion neutralization [20] by water, may also be playing a role, but from the data presented in Figure 6, it is unclear to what extent.

The accumulated intensities of particular anions from FH cells are shown in Figure 5 alongside the intensities

from FD and FF cells. Well-preserved, hydrated cells should have a similar amount of these species as FD cells, yet the observed SI intensities were significantly lower ( $p < 0.05$ ) for all but  $OH^-$ . Incorporated water plays an important role in determining the yield of negatively charged monatomic species. Water ice drastically reduced the SI yields of negative ions compared to positive monatomic ions in computational studies [59,60], and this may explain why the SI intensities were lower in the FH cells. The insignificant decrease in the  $OH^-$  intensity was not surprising as it is a water fragment. Protons donated by the intracellular water may also combine with the anions to form neutral, undetected species.

A representative depth profile from a sample with frozen-hydrated cells is shown in Additional file 2: Figure S2 C, depicting the Poisson-corrected intensity of selected secondary ions as a function of  $C_{60}^{++}$  sputter time.  $H_2O^+$  and  $H_5O_2^+$  profiles are shown in addition to the same fragment profiles shown in Additional file 2: Figure S2 A and B. As before, qualitatively the intensity profiles of the organic molecules are similar to those observed from the FD and FF cells. Although the initial normalized intensities are lower for all of the selected organic molecules, the intensity decay over time appears lower compared to the profiles in Additional file 2: Figure S2 A and B. This is consistent with a lowered damage cross section in the FH depth profile compared to the profiles of the dried cells. Unlike in Additional file 2: Figure S2 A and B, in Figure S2 C the PC headgroup ( $C_5H_{15}PNO_4^+$ ) molecule had a higher initial intensity than the headgroup fragments ( $C_3H_8N^+$  and  $C_5H_{12}N^+$ ). The intensity of  $NH_4^+$

starts and remains high throughout the profile, likely from the ammonium acetate rinsing solution.

Given the data presented above, it would be interesting to further investigate the secondary ion yield increases that may be obtained by first doing chemical fixation to remove diffusible salts ions, and then cryogenic analysis for decreased damage. This experiment would help determine the relative contributions of proton donation from water versus decreased damage from cryogenic temperatures.

## Conclusions

Sample preparation plays a key role in determining the information that is obtained from single cells with ToF-SIMS. The removal of excess media before analysis is necessary, but using rinsing technique that was too aggressive damaged the plasma membrane. The presence of intracellular salts reduced the secondary ion yield an average of 2.6-fold. Chemical fixation followed by rinsing removed a majority of the intracellular salts, “recovering” the positive secondary ion yields.  $\text{Cl}^-$  ion yields were highest in the freeze-dried cells and lowest in the formaldehyde-fixed cells. The data presented here is consistent with anion neutralization as the dominant mechanism for the lower ion yields. All of the organic secondary ions that were detected in the freeze-dried cells were also detected in the formaldehyde-fixed cells. Well-preserved, hydrated cells showed no increase or a decreased yield for most low mass ions, but an increased yield for higher mass fragments. This is consistent with the mechanism where a reduced damage cross section is produced by analysis at cryogenic temperatures. Numerous ions that were detected from the frozen-hydrated cells were not detected from the freeze-dried cells, however many of these ions were attributed to chemical combinations of water, salt and the ammonium acetate rinsing solution.

Future considerations regarding the optimal sample preparation for depth profiling cells would be need to be addressed in a case specific manner (e.g., for experiments that involve mapping small molecule drugs in cells). It may be beneficial (or necessary) to utilize chemical fixation or frozen-hydrated analysis to increase SI yields, but if the molecule is unbound and is removed or relocated during preparation, cryofixation would be necessary for accurate imaging.

## Additional files

**Additional file 1: Figure S1.** (A)  $\text{Na}^+$  peak and (B)  $^{41}\text{K}^+$  peak from the depth profile of FH cells. The  $\text{K}^+/\text{Na}^+$  ratio is 14.7, signifying the cells were well preserved. The  $^{41}\text{K}^+$  isotope peak was used due to detector saturation of the  $^{39}\text{K}^+$  isotope peak.

**Additional file 2: Figure S2.** (A) Depth profile from cells that were freeze-dried. (B) Depth profile from cells that were chemically fixed with formaldehyde. (C) Depth profile from cells that were analyzed frozen-hydrated. The depth profiles were normalized by the  $\text{Bi}_3^+$  ion dose.

**Additional file 3: Table S1.** All positive secondary ions detected from both the FD and FF cells. Sorted by fold difference value, smallest to largest.

**Additional file 4: Table S2.** Positive ions that were detected from the frozen-hydrated cells but not the freeze-dried cells, or in new very low amounts in the FD cells.

**Additional file 5: Table S3.** All positive secondary ions detected from both the FH cells and the FD cells.

## Competing interests

The authors declare that they have no competing interests.

## Authors' contributions

MAR performed the experiments, analyzed the data and created the figures. MAR and DGC developed the experimental design, did the manuscript writing and editing, and approved the final manuscript.

## Acknowledgements

The authors thank NIH and the NIBIB for their financial support (NIH EB-002027) to this work, as well as Dr. Liney Árnadóttir for her technical assistance with the FH sample mounting onto the cold stage. The authors also thank Dr. Buddy Ratner for use of his cell culture facility and Dr. Cecilia Giachelli for the use of her freeze drier.

## Author details

<sup>1</sup>National ESCA and Surface Analysis Center for Biomedical Problems, University of Washington, 98195 Seattle, WAUSA. <sup>2</sup>Department of Chemical Engineering, University of Washington, 98195 Seattle, WA, USA. <sup>3</sup>Department of Bioengineering, University of Washington, 98195 Seattle, WA, USA.

Received: 20 May 2013 Accepted: 20 June 2013

Published: 5 July 2013

## References

1. Fletcher JS (2009) Cellular imaging with secondary ion mass spectrometry. *Analyst* 134:2204–2215
2. Sjøvall P, Johansson B, Belazi D, Stenvinkel P, Lindholm B, Lausmaa J, Schalling M (2008) TOF-SIMS analysis of adipose tissue from patients with chronic kidney disease. *Appl Surf Sci* 255:1177–1180
3. Brison J, Benoit DSW, Muramoto S, Robinson M, Stayton PS, Castner DG (2011) ToF-SIMS imaging and depth profiling of HeLa cells treated with bromodeoxyuridine. *Surf Interface Anal* 43:354–357
4. Barnes CA, Brison J, Robinson M, Graham DJ, Castner DG, Ratner BD (2011) Identifying individual cell types in heterogeneous cultures using secondary ion mass spectrometry imaging with C60 etching and multivariate analysis. *Anal Chem* 84:893–900
5. Magnusson YK, Friberg P, Sjøvall P, Malm J, Chen Y (2008) TOF-SIMS analysis of lipid accumulation in the skeletal muscle of ob/ob mice. *Obesity* 16:2745–2753
6. Muramoto S, Graham DJ, Wagner MS, Lee TG, Moon DW, Castner DG (2011) ToF-SIMS analysis of adsorbed proteins: principal component analysis of the primary ion species effect on the protein fragmentation patterns. *J Phys Chem C* 115:24247–24255
7. Dubey M, Brison J, Grainger DW, Castner DG (2011) Comparison of  $\text{Bi}^+$ ,  $\text{Bi}_3^+$  and  $\text{C}_{60}^+$  primary ion sources for ToF-SIMS imaging of patterned protein samples. *Surf Interface Anal* 43:261–264
8. Graf N, Gross T, Wirth T, Weigel W, Unger WES (2009) Application of XPS and ToF-SIMS for surface chemical analysis of DNA microarrays and their substrates. *Anal Bioanal Chem* 393:1907–1912
9. Lee CY, Harbers GM, Grainger DW, Gamble LJ, Castner DG (2007) Fluorescence, XPS, and TOF-SIMS surface chemical state image analysis of DNA microarrays. *J Am Chem Soc* 129:9429–9438
10. Fisher GL, Belu AM, Mahoney CM, Wormuth K, Sanada N (2009) Three-dimensional time-of-flight secondary ion mass spectrometry imaging of a

- pharmaceutical in a coronary stent coating as a function of elution time. *Anal Chem* 81:9930–9940
11. Belu A, Mahoney C, Wormuth K (2008) Chemical imaging of drug eluting coatings: combining surface analysis and confocal raman microscopy. *J Controlled Release* 126:111–121
  12. Klerk LA, Dankers PYW, Popa ER, Bosman AW, Sanders ME, Reedquist KA, Heeren RMA (2010) TOF-secondary ion mass spectrometry imaging of polymeric scaffolds with surrounding tissue after in vivo implantation. *Anal Chem* 82:4337–4343
  13. Barnes CA, Brison J, Michel R, Brown BN, Castner DG, Badylak SF, Ratner BD (2011) The surface molecular functionality of decellularized extracellular matrices. *Biomaterials* 32:137–143
  14. Gunnarsson A, Kollmer F, Sohn S, Hook F, Sjovald P (2010) Spatial-resolution limits in mass spectrometry imaging of supported lipid bilayers and individual lipid vesicles. *Anal Chem* 82:2426–2433
  15. Muramoto S, Brison J, Castner DG (2012) Exploring the surface sensitivity of TOF-secondary ion mass spectrometry by measuring the implantation and sampling depths of Bi<sub>n</sub> and C<sub>60</sub> ions in organic films. *Anal Chem* 84:365–372
  16. Kurczy ME, Piehowski PD, Willingham D, Molyneux KA, Heien ML, Winograd N, Ewing AG (2010) Nanotome cluster bombardment to recover spatial chemistry after preparation of biological samples for SIMS imaging. *J Am Soc Mass Spectrom* 21:833–836
  17. Kurczy ME, Piehowski PD, Parry SA, Jiang M, Chen G, Ewing AG, Winograd N (2008) Which is more important in bioimaging SIMS experiments—the sample preparation or the nature of the projectile? *Appl Surf Sci* 255:1298–1304
  18. Chandra S (1986) Imaging intracellular elemental distribution and ion fluxes in cultured cells using ion microscopy: a freeze-fracture methodology. *J Microsc* 144:15–37
  19. Roddy TP, Cannon DM, Ostrowski SG, Winograd N, Ewing AG (2002) Identification of cellular sections with imaging mass spectrometry following freeze fracture. *Anal Chem* 74:4020–4026
  20. Piwowar AM, Lockyer NP, Vickerman JC (2009) Salt effects on ion formation in desorption mass spectrometry: an investigation into the role of alkali chlorides on peak suppression in time-of-flight-secondary ion mass spectrometry. *Anal Chem* 81:1040–1048
  21. Jones EA, Lockyer NP, Vickerman JC (2008) Depth profiling brain tissue sections with a 40 keV C-60(+) primary ion beam. *Anal Chem* 80:2125–2132
  22. Berman ESF, Fortson SL, Checchi KD, Wu L, Felton JS, Wu KJ, Kulip KS (2008) Preparation of single cells for imaging/profiling mass spectrometry. *J Am Soc Mass Spectrom* 19:1230–1236
  23. Nygren H, Eriksson C, Malmberg P, Sahlin H, Carlsson L, Lausmaa J, Sjovald P (2003) A cell preparation method allowing subcellular localization of cholesterol and phosphocholine with imaging TOF-SIMS. *Colloids Surf B Biointerphases* 30:87–92
  24. Malm J, Giannaras D, Riehle MO, Gadegaard N, Sjovald P (2009) Fixation and drying protocols for the preparation of cell samples for time-of-flight secondary ion mass spectrometry analysis. *Anal Chem* 81:7197–7205
  25. Passarelli MK, Winograd N (2011) Characterizing in situ glycerophospholipids with SIMS and MALDI methodologies. *Surf Interface Anal* 43:269–271
  26. Breitenstein D, Rommel CE, Stolwijk J, Wegener J, Hagenhoff B (2008) The chemical composition of animal cells reconstructed from 2D and 3D ToF-SIMS analysis. *Appl Surf Sci* 255:1249–1256
  27. Breitenstein D, Rommel CE, Mollers R, Wegener J, Hagenhoff B (2007) The chemical composition of animal cells and their intracellular compartments reconstructed from 3D mass spectrometry. *Angew Chem Int Ed* 46:5332–5335
  28. Chandra S, Ausserer WA, Morrison GH (1987) Evaluation of matrix effects in ion microscopic analysis in freeze-fractured, freeze-dried cultured cells. *J Microsc* 148:223–239
  29. Fartmann M, Kriegeskotte C, Dambach S, Wittig A, Sauerwein W, Arlinghaus HF (2004) Quantitative imaging of atomic and molecular species in cancer cultures with TOF-SIMS and Laser-SNMS. *Appl Surf Sci* 231:428–431
  30. Lanekoff I, Kurczy ME, Adams KL, Malm J, Karlsson R, Sjovald P, Ewing AG (2011) An in situ fracture device to image lipids in single cells using ToF-SIMS. *Surf Interface Anal* 43:257–260
  31. Clerc J, Fourre C, Fragu P (1997) SIMS microscopy: methodology, problems and perspectives in mapping drugs and nuclear medicine compounds. *Cell Biol Int* 21:619–633
  32. Kellenberger E (1987) The response of biological macromolecules and supramolecular structures to the physics of specimen cryopreparation. In: Steinbrecht RA, Zierold K (eds) *Cryotechniques in biological electron microscopy*. Springer-Verlag, Berlin
  33. Fletcher JS, Rabbani S, Henderson A, Lockyer NP, Vickerman JC (2011) Three-dimensional mass spectral imaging of HeLa-M cells - sample preparation, data interpretation and visualisation. *Rapid Commun Mass Spectrom* 25:925–932
  34. Frisz JF, Lou K, Klitzing HA, Hanafin WP, Lizunov V, Wilson RL, Carpenter KJ, Kim R, Hutcheon ID, Zimmerberg J, Weber PK, Kraft ML (2013) Direct chemical evidence for sphingolipid domains in the plasma membranes of fibroblasts. *Proc Natl Acad Sci USA* 110:E613–E622
  35. Mahoney CM, Fahey AJ, Gillen G, Xu C, Batteas JD (2007) Temperature-controlled depth profiling of poly(methyl methacrylate) using cluster secondary ion mass spectrometry. 2. Investigation of sputter-induced topography, chemical damage, and depolymerization effects. *Anal Chem* 79:837–845
  36. Mahoney CM, Fahey AJ, Gillen G (2007) Temperature-controlled depth profiling of poly(methyl methacrylate) using cluster secondary ion mass spectrometry. 1. Investigation of depth profile characteristics. *Anal Chem* 79:828–836
  37. Piwowar AM, Fletcher JS, Kordys J, Lockyer NP, Winograd N, Vickerman JC (2010) Effects of cryogenic sample analysis on molecular depth profiles with TOF-secondary ion mass spectrometry. *Anal Chem* 82:8291–8299
  38. Piehowski PD, Kurczy ME, Willingham D, Parry S, Heien ML, Winograd N, Ewing AG (2008) Freeze-etching and vapor matrix deposition for ToF-SIMS imaging of single cells. *Langmuir* 24:7906–7911
  39. Lewis KB, Ratner BD (1993) Observation of surface rearrangement of polymers using ESCA. *J Colloid Interface Sci* 159:77–85
  40. Ratner BDW PK, Hoffman AS, Kelly MA, Scharpen LH (1978) Radiation-grafted hydrogels for biomaterial applications as studied by the ESCA technique. *J Appl Polym Sci* 22:643–664
  41. Rabbani S, Fletcher JS, Lockyer NP, Vickerman JC (2011) Exploring subcellular imaging on the buncher-ToF J105 3D chemical imager. *Surf Interface Anal* 43:380–384
  42. Moller J, Beumer A, Lipinsky D, Arlinghaus HF (2006) Introduction of a cryosectioning-ToF-SIMS instrument for analysis of non-dehydrated biological samples. *Appl Surf Sci* 252:6709–6711
  43. Lanekoff I, Kurczy ME, Hill R, Fletcher JS, Vickerman JC, Winograd N, Sjovald P, Ewing AG (2010) Time of flight mass spectrometry imaging of samples fractured in situ with a spring-loaded trap system. *Anal Chem* 82:6652–6659
  44. Wittig A, Wiemann M, Fartmann M, Kriegeskotte C, Arlinghaus HF, Zierold K, Sauerwein W (2005) Preparation of cells cultured on silicon wafers for mass spectrometry analysis. *Microsc Res Tech* 66:248–258
  45. Piwowar AM, Keskin S, Delgado MO, Shen K, Hwe JJ, Lanekoff I, Ewing AG, Winograd N (2013) C60-ToF SIMS imaging of frozen hydrated HeLa cells. *Surf Interface Anal* 45:302–304
  46. Brison J, Muramoto S, Castner DG (2010) ToF-SIMS depth profiling of organic films: a comparison between single-beam and dual-beam analysis. *J Phys Chem C* 114:5565–5573
  47. Tahallah N, Brunelle A, De La Porte S, Laprevote O (2008) Lipid mapping in human dystrophic muscle by cluster-time-of-flight secondary ion mass spectrometry imaging. *J Lipid Res* 49:438–454
  48. Passarelli MK, Winograd N (2011) Lipid imaging with time-of-flight secondary ion mass spectrometry (ToF-SIMS). *Biochim Biophys Acta* 1811:976–990
  49. Altelaar AFM, Klinkert I, Jalink K, De Lange RPJ, Adan RAH, Heeren RMA, Piersma SR (2005) Gold-enhanced biomolecular surface imaging of cells and tissue by SIMS and MALDI mass spectrometry. *Anal Chem* 78:734–742
  50. Castner DG, Ratner BD (2002) Biomedical surface science: foundations to frontiers. *Surf Sci* 500:28–60
  51. Lanekoff I, Kurczy ME, Hill R, Fletcher JS, Vickerman JC, Winograd N, Sjovald P, Ewing AG (2010) Time of flight mass spectrometry imaging of samples fractured in situ with a spring-loaded trap system. *Anal Chem* 82:6652–6659
  52. Robinson MA, Graham DJ, Castner DG (2012) ToF-SIMS depth profiling of cells: z-correction, 3D imaging, and sputter rate of individual NIH/3T3 fibroblasts. *Anal Chem* 84:4880–4885
  53. Fletcher JS, Lockyer NP, Vickerman JC (2011) Developments in molecular SIMS depth profiling and 3D imaging of biological systems using polyatomic primary ions. *Mass Spectrom Rev* 30:142–174
  54. Sostarecz AG, Cannon DM, Mcquaw CM, Sun S, Ewing AG, Winograd N (2004) Influence of molecular environment on the analysis of phospholipids by time-of-flight secondary ion mass spectrometry. *Langmuir* 20:4926–4932
  55. Vaezian B, Arderton CR, Kraft ML (2010) Discriminating and imaging different phosphatidylcholine species within phase-separated model

membranes by principal component analysis of TOF-secondary ion mass spectrometry images. *Anal Chem* 82:10006–10014

56. Mantus DS, Ratner BD, Carlson BA, Moulder JF (1993) Static secondary ion mass spectrometry of adsorbed proteins. *Anal Chem* 65:1431–1438
57. Lhoest JB, Wagner MS, Tidwell CD, Castner DG (2001) Characterization of adsorbed protein films by time of flight secondary ion mass spectrometry. *J Biomed Mater Res* 57:432–440
58. Conlan XA, Lockyer NP, Vickerman JC (2006) Is proton cationization promoted by polyatomic primary ion bombardment during time-of-flight secondary ion mass spectrometry analysis of frozen aqueous solutions? *Rapid Commun Mass Spectrom* 20:1327–1334
59. Wojciechowski IA, Kutliev U, Sun S, Szakal C, Winograd N, Garrison BJ (2004) Emission of ionic water clusters from water ice films bombarded by energetic projectiles. *Appl Surf Sci* 231–232:72–77
60. Wojciechowski IA, Sun S, Szakal C, Winograd N, Garrison BJ (2004) Ion emission from water ice due to energetic particle bombardment. *J Phys Chem A* 108:2993–2998

doi:10.1186/1559-4106-8-15

**Cite this article as:** Robinson and Castner: Characterization of sample preparation methods of NIH/3T3 fibroblasts for ToF-SIMS analysis. *Biointerphases* 2013 **8**:15.

**Submit your manuscript to a SpringerOpen<sup>®</sup> journal and benefit from:**

- ▶ Convenient online submission
- ▶ Rigorous peer review
- ▶ Immediate publication on acceptance
- ▶ Open access: articles freely available online
- ▶ High visibility within the field
- ▶ Retaining the copyright to your article

---

Submit your next manuscript at ▶ [springeropen.com](http://springeropen.com)

---